ELSEVIER

Biophysical Chemistry 79 (1999) 219–229

Biophysical Chemistry

Electrochemical generation of ferrylmyoglobin during oxidation of styrene with films of DNA and a poly(ester sulfonic acid) ionomer

Jilie Kong[a,*], Jeremiah N. Mbindyo[b], Xingliang Wu[a], Jack X. Zhou[c], James F. Rusling[b]

[a] *Department of Chemistry, Fudan University, Shanghai 200433, China*
[b] *Department of Chemistry, University of Connecticut, U-60, 55 N. Eagleville Rd., Storrs, CT 06269-3060, USA*
[c] *CVI Spectral Instruments, Putnam, CT 06260, USA*

Received 3 February 1999; received in revised form 6 April 1999; accepted 6 April 1999

Abstract

The chemistry of electrochemically-driven myoglobin-catalyzed oxidation of styrene was investigated in films of DNA or Eastman AQ ionomer on optically transparent electrodes. Conversion of styrene to styrene oxide proceeded via a ferrylmyoglobin radical intermediate. Ferrylmyoglobins were clearly detected by spectroelectrochemistry in films of 1–4 mm thick. The ferrylmyoglobin radical is produced by reaction of metmyoglobin (Mb) in the films with hydrogen peroxide formed by electrochemical catalytic reduction of oxygen catalyzed by Mb. Thus, electrochemically-driven styrene oxidation with these films proceeds by a 'doubly catalytic' electrode-driven reduction–oxidation pathway. Ferrylmyoglobin formation during electrolysis of Mb–DNA films in aerobic solutions was much faster, and styrene oxidation occurred with less Mb decomposition compared to the Mb–AQ films. The better performance of Mb–DNA films is correlated with a larger fraction of electroactive Mb and better stability than for the Mb–AQ films.

Keywords: Myoglobin; DNA; Ferrylmyoglobin; Electrochemical generation; Protein films

1. Introduction

While the main function of myoglobin (Mb) in mammals is to transport oxygen, it also catalyzes oxidations of organic molecules [1–8] The active oxidant in these processes can be formed by reacting metmyoglobin [X–MbFe(III)] with hydrogen peroxide [Eq. (1)] [9–12]

$$\text{X–MbFe(III)} + H_2O_2 \rightarrow {}^{\bullet}\text{X–MbFe(IV)}{=}O + H_2O \quad (1)$$

* Corresponding author. Tel.: +86-21-65642405; fax: +86-21-65641740.
E-mail address: jkong@fudan.ac.cn (J. Kong)

0301-4622/99/$ - see front matter
PII: S0301-4622(99)00055-1

Here, $^{\bullet}$X–MbFe(IV)=O represents the active ferrylmyoglobin radical which oxidizes olefins by oxygen transfer. One oxygen from H_2O_2 becomes bound to the iron of X–MbFe(III), while the second oxidizing equivalent creates a free radical on an amino acid residue (X) near the protein surface [1–4,8,13,14]. Low spin Fe(IV)=O heme in ferrylmyoglobin was clearly identified by Raman, X-ray absorption, Mossbauer, and NMR spectroscopies [15–19]. Ferrylmyoglobin radical has a lifetime of 30 s at pH 7 and room temperature [4,11,20]. This radical decays via Eq. (2) and other possible pathways [10–12] to the relatively stable HX–MbFe(IV)=O, a non-radical ferrylmyoglobin, which we will also refer to as MbFe(IV)=O.

$$2^{\bullet}\text{X–MbFe(IV)=O} + H_2O_2 \rightarrow 2\text{HX–MbFe(IV)=O} + O_2 \quad (2)$$

Ferrylmyoglobin radical may be involved in disease-causing chemical events and has been implicated in oxidative cellular damage in coronary heart disease [5,20–23].

Catalytic reactions of Mb have some similarities to those of human liver cytochrome P450s (cyt P450), which are thought to catalyze oxidative carcinogenic activation of lipohilic drugs and pollutants [24,25]. As proposed for cyt P450, Mb employs a high valent heme iron-oxo complex to oxidize substrates. While the active intermediate is highly unstable for cyt P450s, ferrylmyoglobin and ferrylmyoglobin radical can be detected by visible absorption spectroscopy [22,23].

Using spectroelectrochemistry of Mb dissolved in solutions and microemulsions containing oxygen, we previously showed that ferrylmyoglobin radical can be generated by electrolytic reduction [26]. Thus, electrolysis could also be used to drive Mb-mediated oxidation of styrene to styrene oxide. These oxidations are 'doubly catalytic', featuring catalytic electrochemical *reduction* of Mb-bound dioxygen to hydrogen peroxide, followed by peroxide-initiated ferrylmyoglobin radical formation and catalytic *oxidation* of the olefinic bond.

We recently showed that Mb and cyt P450cam in ultrathin films of polyions on electrodes [27] were much more active than the proteins in solution for aerobic electrochemically driven styrene oxidation. These films were formed layer by layer and typically contain two layers of electroactive protein. Positively charged Mb binds to polyanionic layers by coulombic interactions. However, the film thickness of 10–12 nm is too small to obtain sufficient optical absorbance for spectroelectrochemical studies of the Mb intermediates.

In this paper, we report electrochemical and spectroelectrochemical studies in 1–4-μm thick Mb-polyion films on transparent electrodes. Characteristic spectra of ferrylmyoglobin were found during electrochemically-driven catalytic styrene oxidation using these films.

2. Experimental

2.1. Materials and solutions

Lyophilized horse heart myoglobin from Sigma was dissolved in buffer and filtered through 30 000-MW cutoff Amicon filters to remove higher MW impurities. The effectiveness of purification was confirmed by PAGE [28]. Poly(ester sulfonic acid) sodium ionomer, Eastman AQ 38 (MW = 14 000, $T_g = 38^{\circ}C$, 11% sulfonates per monomer) was a gift from Eastman Chemical Co.

Optically transparent electrodes were 3×0.5-cm glass slides coated with indium tin oxide (ITO, resistance 10 Ω cm^{-1}, CG-80IN-CUV from Delta Technologies, Stillwater, MI). Water was purified to specific resistance 18 MΩ-cm using a Barnstead Nanopure water purification system. Quantofix peroxide 100 test sticks from Macherey-Nagel GMBH & Co., Germany were used to estimate hydrogen peroxide concentrations in solution.

Highly polymerized DNA (MW approx. 1×10^8, Sigma) was purified as follows: 10 mM DNA in 10 mM TRIS–HCl buffer, pH 7.4, containing 1 mM EDTA was precipitated with 2 volumes ethanol ($-20^{\circ}C$), collected by centrifugation, then re-dissolved in the pH 7.4 TRIS/EDTA buffer. This solution was passed through a 0.2-μm Sep-Pak cartridge, then dialyzed with 12 000 MW cutoff

tubing against 400 volumes water for 48 h. Final DNA concentration was 1 mg ml^{-1}, determined from optical absorbance at 260 nm assuming 50 μg DNA yields A_{260} of 1.0 in 1.0-ml buffer with a 1-cm light path [29].

2.2. Apparatus and procedures

Films were prepared by evenly spreading known volumes of appropriate mixtures of Mb and DNA or AQ polymer in buffer on an electrode of choice, and drying in air in a covered container. Film thicknesses were estimated from amounts and densities of materials deposited. Mb–DNA films on conducting ITO glass slides were made from 30 μl 1 mg ml^{-1} Mb and 20 μl 1 mg ml^{-1} DNA, giving layers approximately 0.3 μm thick. Additional layers were deposited on electrodes to obtain sufficient optical absorbance for a particular experiment. Final film thicknesses were between 0.6 and 1.2 μm.

Before coating with AQ ionomer, ITO electrodes were washed successively with ethanol, water and 1% acetic acid. The last step introduces positive charge on the ITO surface and improves adhesion of the negative AQ polymer. Electrodes were then rinsed with water and dried. Eastman AQ 38 at 1 mg ml^{-1} in water was sonicated overnight to provide a uniform translucent dispersion. A 1:1 (v/v) mixture of AQ dispersion and 0.12 mM Mb (2 mg ml^{-1}) in pH 7 TRIS buffer was deposited onto the ITO electrodes at 100 μl cm^{-2}. Coated electrodes were covered and allowed to evaporate to near dryness, after which two more coatings were applied. Final film thickness was estimated at 3.5 mm. These films were made thicker than the Mb–DNA films to insure sufficient electroactivity, since previous work showed that only 10% of the Mb deposited was electroactive [30]. Furthermore, approximately 40% of the Mb deposited is leached into solution during initial equilibration, after which the films are stable. Thus, Mb–AQ films were first equilibrated with buffer solution, then removed and placed in fresh buffer before the start of an experiment.

Similar procedures were used to prepare films of Mb and DNA or AQ on pyrolytic graphite and carbon cloth electrodes. These electrodes were used in comparative electrolysis studies of the Mb-mediated electrochemical oxidation of styrene. Gas chromatographic analysis of product mixtures was done with a procedure described previously [26,27].

A Bioanalytical Systems BAS-100B/W electrochemical analyzer was used for cyclic voltammetry (CV). The three electrode thermostated cells employed a saturated calomel reference electrode (SCE) and a Pt wire counter electrode. Working electrodes were ITO or basal plane pyrolytic graphite (PG), with electrodes prepared as described previously [26]. CV peak currents were obtained by the conventional method of linearly extrapolating the baseline before the peak and subtracting. The buffer for voltammetry and spectroelectrochemistry was pH 7, 10 mM TRIS–HCl + 50 mM NaBr. Solutions were purged with gentle streams of nitrogen, argon, or oxygen as required. Ohmic drop of cells was $> 95\%$ compensated.

The cell potential in spectroelectrochemistry was controlled by the BAS-100B/W, or by a Princeton Applied Research PARC M273 potentiostat. The spectroelectrochemical cell was a conventional 1-cm quartz cuvette in which coated transparent ITO electrodes were inserted perpendicular to the light path. Pt wire counter and micro reference (SCE or saturated Ag/AgCl) electrodes were placed in the cell solution, but out of the light path [26]. Absorbance spectra were collected at fixed applied potentials by using an SM-210 CCD spectrophotometer (CVI Spectral Instruments, Putnam, CT, USA) or a Perkin-Elmer Lambda-6 spectrophotometer. Spectra were recorded against AQ- or DNA-coated ITO electrodes as references.

3. Results

3.1. Cyclic voltammetry

The heme Fe(III)/Fe(II) redox couple of Mb was previously shown to give reversible voltammetry in AQ films on pyrolytic graphite (PG) electrodes [30]. Fig. 1 shows chemically reversible

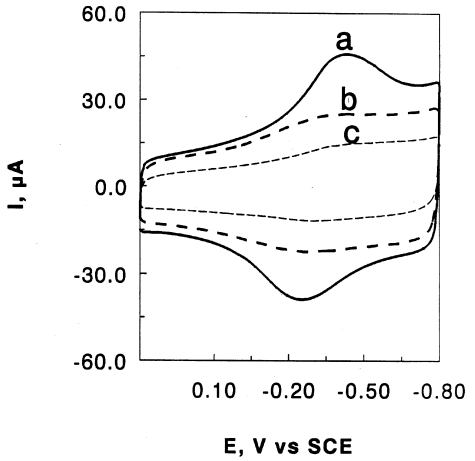

Fig. 1. Cyclic voltammograms at 1.5 V s^{-1} in anaerobic pH 7 TRIS buffer: (a) Mb–AQ film on ITO electrode; (b) 0.3 mM Mb in solution at bare ITO electrode; (c) ITO electrode in buffer without Mb. (In all CV, reduction currents are positive and oxidation currents are negative).

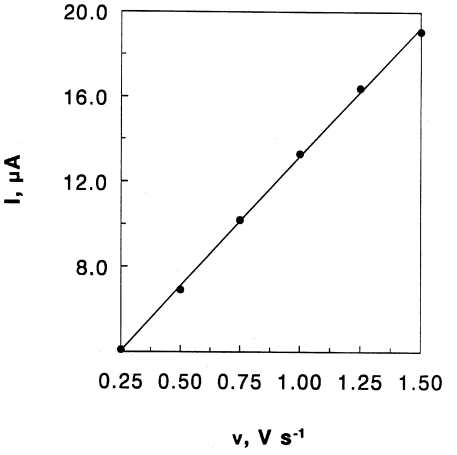

Fig. 2. Influence of scan rate on Fe(III) reduction peak current for Mb–AQ/ITO films in pH 7 buffer.

oxidation–reduction peaks for Mb heme Fe(III)/Fe(II) in a Mb–AQ film on an ITO electrode. Peaks in the AQ film are larger and better defined than for Mb in solution on a bare ITO electrode. Oxidation and reduction peak currents are nearly equal, and are directly proportional to scan rate (Fig. 2). These CV results are characteristic [31] of reversible electrochemical interconversion of Fe(III) and Fe(II) forms of the protein in the thin Mb–AQ film on the electrode.

We previously showed that Mb in films of double stranded (ds) calf thymus (CT) DNA of av. MW 10^6 gave chemically reversible heme Fe(III)/Fe(II) electrochemistry on PG electrodes [32], with similar voltammetric characteristics to those described above for Mb–AQ. In this work, we found that ds CT DNA with av. MW 10^8 gave somewhat more stable films (> 1 week in buffer) than the lower MW DNA, with similar chemically reversible thin-layer electrochemical characteristics of Mb on PG and ITO electrodes.

Since electrochemical catalytic reduction of oxygen is essential to activate Mb for catalytic oxidations [26], we also examined the influence of oxygen on CVs of the films. The typical reversible CVs found in anaerobic solutions are significantly transformed when oxygen is added to the solution. Changes include a large increase in the Fe(III) reduction peak, and a disappearance of the Fe(II) oxidation peak (Fig. 3). This is similar in both DNA and AQ films. The new large reduction peak is approximately 300 mV more positive than the direct reduction peak of oxygen using electrodes coated with films not containing Mb.

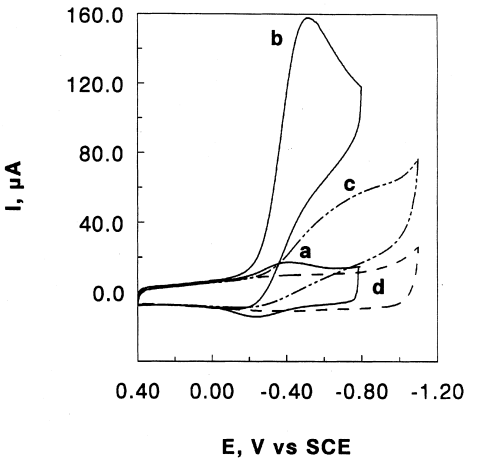

Fig. 3. Cyclic voltammograms at 0.5 V s^{-1} in 5 ml pH 7 buffer for: (a) Mb–AQ film on ITO electrode, solution purged with nitrogen; (b) same electrode after injecting 20-ml oxygen into buffer; (c) AQ film with no Mb on ITO electrode after injecting 20-ml oxygen into buffer; (d) AQ film with no Mb on ITO electrode, buffer purged with nitrogen.

3.2. Spectroelectrochemistry

Visible absorption spectra of ferrylmyoglobin have been well characterized and interpreted in the medium pH range [22,23,26]. Fig. 4 presents standard solution spectra of species likely to be involved during electrolysis of Mb films. Metmyoglobin has an iron heme Soret band at 408 nm, and smaller bands at 503 and 631 nm. Both MbFe(II)–O_2 and $^{\bullet}$X–MbFe(IV)=O have Soret bands at longer wavelengths than metmyoglobin. MbFe(IV)=O and $^{\bullet}$X–MbFe(IV)=O are detected simultaneously by the Soret band at 421 nm and characteristic bands at 548 and 584 nm after addition of hydrogen peroxide to metmyoglobin (Fig. 4b). MbFe(IV)=O and $^{\bullet}$X–MbFe(IV)=O cannot be distinguished from their visible spectra, and $^{\bullet}$X–MbFe(IV)=O decays [Eq. (2)] to MbFe(IV)=O in 30 s [4,11,20]. MbFe(II)–O_2 bands at 540 and 580 nm have smaller band widths than bands of ferrylmyoglobins in the same wavelength range.

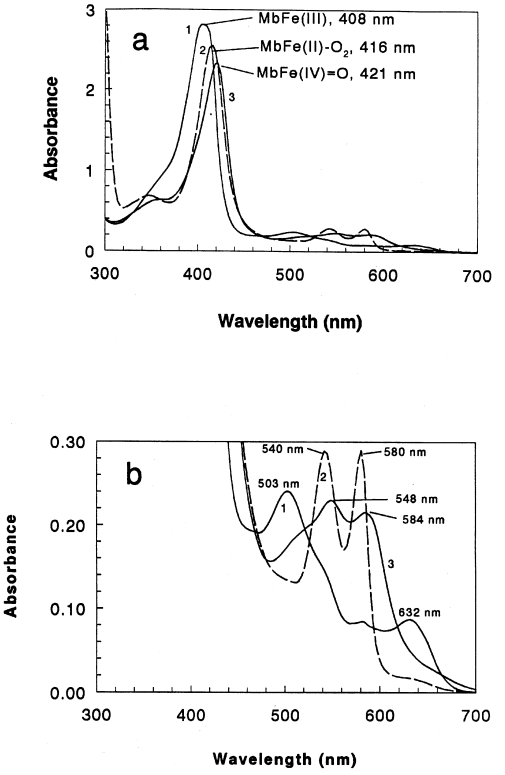

Fig. 4. Standard absorbance spectra of various forms of Mb in aerobic pH 7 buffer: (a) full spectral range including Soret bands; (b) higher sensitivity to view bands in the 450–700-nm region. Samples are (1) 30 mm MbFe(III); (b) MbFe(II)–O_2 formed by adding 17 mM ascorbic acid to 30 mm MbFe(III), and (3) MbFe(IV)=O formed by adding 0.6 mM hydrogen peroxide to 30 μm MbFe(III). See Onuoha et al. [26] for details.

Visible absorbance spectra of Mb–AQ films (Fig. 5a) were similar to spectra of Mb in solution. The Soret band appeared at 409 nm. The bands at 503 and 632 nm are observed for Mb–AQ (Fig. 5b), but spectral shape in this region was slightly different than for metmyoglobin in solution. Electrolysis for 40 min at an applied voltage negative of the MbFe(III) reduction peak in the presence of oxygen gradually converted the 409-nm Soret band to 421 nm, characteristic of ferrylmyoglobins. The spectrum also developed bands at 548 and 580 nm.

When Mb–AQ films were electrolyzed in solu-

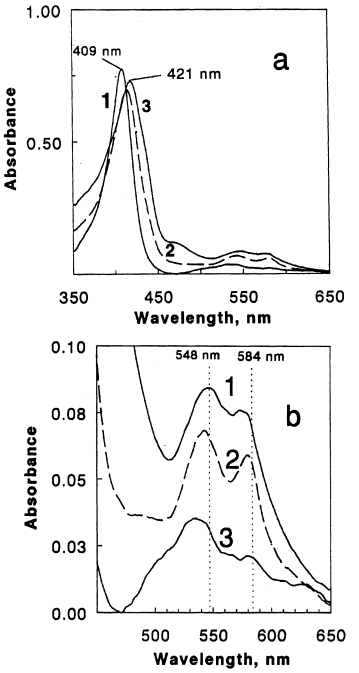

Fig. 5. Absorbance spectra of Mb–AQ films on ITO electrodes in aerobic pH 7 buffer: (a) full spectral range including Soret bands; (b) at higher sensitivity to view bands in the 450–650-nm region. Samples are (1) before electrolysis; (2) after 20-min electrolysis at −0.6 V vs. SCE; and (3) after 40-min electrolysis at −0.6 V.

tions saturated in styrene (approx. 10 mM) and oxygen, the observed spectral changes were much slower than in the absence of styrene (Fig. 6). Even after 60 min, the 409 metmyoglobin peak was still predominant, and 2 h electrolysis was required to observe the band at 421 nm, accompanied by a shoulder at 409 nm. The spectrum in the 500–600-nm region was indistinct after 2 h electrolysis, and did not specifically confirm the presence of ferrylmyoglobins.

Spectra of Mb–DNA films (Fig. 7a) were nearly identical to spectra of Mb in solution. Here, the Soret band appeared at 408 nm, and bands at 503 and 632 nm were clearly observed (Fig. 7b) in the same shape as in solution (cf. Fig. 4b). Electrolysis at −0.6 V converted the 408-nm band to 421 nm within 10 min, and the characteristic ferrylmyoglobin bands at 548 and 584 nm were clearly observed after only 5-min electrolysis.

During electrolysis of Mb–DNA in the presence of styrene and oxygen, maximum Soret band absorbance at 409 nm occurred in the early stages of the experiment. After a few minutes, the 409 nm absorbance is approximately 0.75, and after 20 min decreased to approximately 0.6 (Fig. 8). Peaks at 503 and 632 nm during the early stages of electrolysis confirm the main absorbing species as

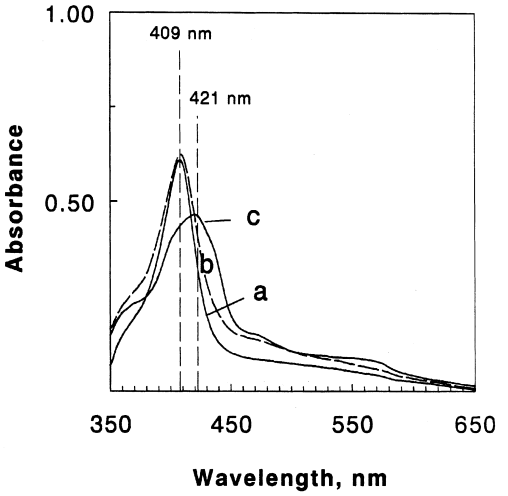

Fig. 6. Absorbance spectra of Mb–AQ films on ITO electrodes in aerobic pH 7 buffer saturated with styrene: (a) before electrolysis; (b) after 60 min-electrolysis at −0.6 V; (c) after 120-min electrolysis at −0.6 V.

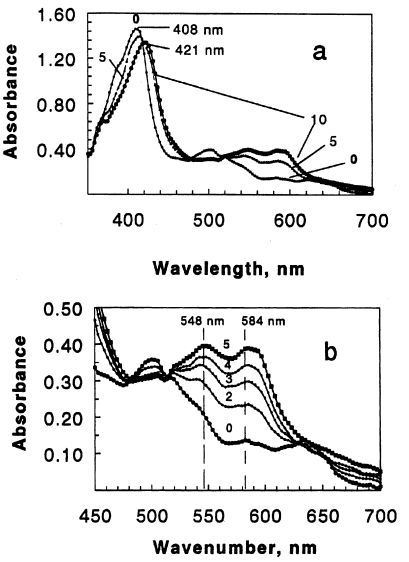

Fig. 7. Absorbance spectra of Mb–DNA films on ITO electrodes in aerobic pH 7 buffer: (a) full spectral range including Soret bands; (b) at higher sensitivity to view bands in the 450–700-nm region. Curves are labeled with minutes of electrolysis at −0.6 V vs. SCE.

metmyoglobin. Between 20 and 60 min, the 409-, 503- and 632-nm peaks are gradually replaced by peaks at 421, 548, and 584 nm, characteristic of ferrylmyoglobins. At 60 min, the applied potential was changed to −0.1 V, where reduction of metmyoglobin and O_2 do not occur. Between 60 and 120 min, the peaks at 421, 548, and 584 nm are slowly replaced by the metmyoglobin peaks at 409, 503 and 632 nm.

3.3. Styrene oxidation

Electrolyses for 1 or 4 h at −0.6 V vs. SCE in pH 7 buffer solutions containing approximately 10 mM styrene under oxygen using Mb–DNA or Mb–AQ films produced styrene oxide and benzaldehyde as products. Styrene oxide is the Mb-catalyzed oxidation product, while benzaldehyde is produced mainly by reaction of styrene with hydrogen peroxide [1–4]. These products were produced with both types of films on carbon cloth, pyrolytic graphite or ITO electrodes. Yields of styrene oxide were two to fourfold larger compared to control electrolyses using the same elec-

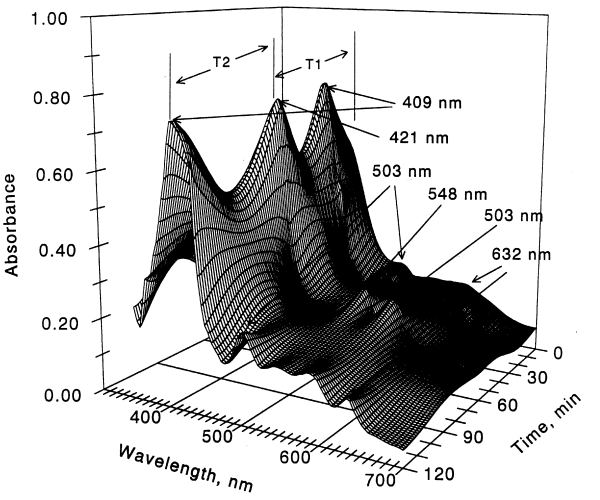

Fig. 8. Time-resolved spectra of a Mb–DNA film on an ITO electrode during electrolysis electrodes in aerobic pH 7 buffer saturated with styrene. Applied potential was −0.6 V (vs. SCE) for period T_1, 0–60 min, then the potential was changed to −0.1 V during T_2, 60–120 min.

trode material in the same solution with no protein coating. For example, a Mb–AQ film on carbon cloth in pH 7 buffer containing oxygen and 10 mM styrene gave 83 nmol styrene oxide after 1 h electrolysis, compared to 25 nmol styrene oxide in the control with no Mb. These typical results showed that the Mb–polyion films in this study have qualitatively similar catalytic behavior to thinner Mb–polyion films grown layer by layer [27]. Detailed studies of catalytic Mb film activity and pathways for oxidations for oxidations of olefins will be reported elsewhere [33].

As for ultrathin, layered Mb–polyion films [27], significantly more hydrogen peroxide was found in solutions after 1 h electrolyses with the Mb–polyion films than in control electrolyses with uncoated electrodes. In the example given above for the Mb–AQ film, 0.35 mg ml^{-1} H_2O_2 was found after 1 h electrolysis, compared to approximately 0.1 mg ml^{-1} H_2O_2 in the bare electrode control electrolysis. These results confirm that Mb is an electrochemical mediator for reduction of O_2 to H_2O_2.

Mb–DNA films on both ITO and PG electrodes produced much more H_2O_2 than the controls during electrolysis in the absence of styrene (Fig. 9). Concentrations of hydrogen peroxide increased for approximately 34–40 min. The concentration of H_2O_2 remained nearly constant after reaching a broad plateau, with only slight decreases afterwards in the absence of styrene. However, when excess styrene was added after 120-min electrolysis, the concentration of H_2O_2 decreased to low levels over the next 120 min (Fig. 9b,c).

4. Discussion

Cyclic voltammetry on ITO electrodes showed that electrochemical conversion of the heme Fe(III) to Fe(II) of Mb was accomplished reversibly in both types of films (Figs. 1 and 2). Chemical reversibility and signal to background ratio in voltammetry is much improved over that of Mb in solution on bare ITO electrodes (Fig. 1). Electrochemical reversibility in the films is similar to that in ultrathin layered polyion films [27], and in films of insoluble surfactants and lipids on electrodes [34]. Possible reasons for the improved Fe(III)/Fe(II) electrochemistry in the films include the relatively high concentration of Mb

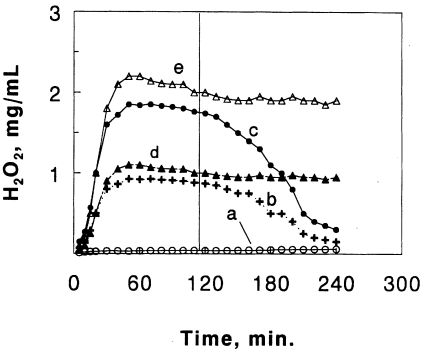

Fig. 9. Influence of electrolysis time at −0.6 V vs. SCE in aerobic pH 7 buffer on concentration of hydrogen peroxide using the following cathodes and conditions: (a) bare PG ($A = 0.79$ cm^2) [bare ITO gave similar results]; (b) Mb–DNA film on PG; 10 mM styrene added at 120 min; (c) Mb–DNA film on ITO, 10 mM styrene added at 120 min; (d) Mb–DNA film on PG, no styrene; and (e) Mb–DNA film on ITO, no styrene.

close to the electrode, and inhibition of adsorption and denaturation of proteins on electrodes by adsorbed ionic film components [28].

Voltammetry of both types of films on ITO electrodes in anaerobic solutions is fully consistent with that found for similar films on pyrolytic graphite and gold electrodes [30,32]. These previous studies showed that Mb–DNA (MW 10^6) films were reasonably stable for up to a week in buffer, and that approximately 40% of the Mb in the film was electroactive at pH 7. Mb–AQ films form hydrogels in water, but only approximately 10% of the Mb deposited was electroactive. Furthermore, when the film is first exposed to water approximately 40% of the original Mb is leached from the film in 2 h, after which the films showed an extended period of stability. That is why Mb–AQ films in the present work were pre-equilibrated with water, then removed and placed into fresh buffer before experiments began.

Voltammetry of Mb films with oxygen in the solution (Fig. 3) is consistent with reduction of oxygen mediated by the protein to give hydrogen peroxide. The increased Fe(III) reduction current in oxygen-containing as opposed to anaerobic solutions, concurrent with the disappearance of the Fe(II) oxidation peak, are consistent with the known rapid reaction of MbFe(II) with O_2 to give MbFe(II)–O_2, followed by reduction of MbFe(II)–O_2 to give H_2O_2, as documented for Mb in solutions and microemulsions [26]. Detection of significantly more H_2O_2 after electrolysis using either Mb film compared to electrolyses without Mb (Fig. 9), is also consistent with Mb-mediated reduction of O_2.

Both types of films catalyzed electrochemically-driven oxidation of styrene to styrene oxide. Results are similar to those with Mb in surfactant and layered polyion films on electrodes [27,33]. In the latter work, we found that addition of catalase to destroy H_2O_2 in electrolysis solutions greatly inhibits styrene oxide formation. Thus, in all these systems, H_2O_2 is necessary for efficient styrene oxidation.

Visible absorbance spectra of MbFe(III) in Mb–DNA films (Fig. 7) were nearly identical to that of MbFe(III) in solution (Fig. 4). Based on spectroelectrochemical results in the absence of styrene, Mb–DNA films cleanly form ferrylmyoglobins during electrolysis at -0.6 V vs. SCE in < 10 min. Spectra after 5–10-min electrolysis (Fig. 7) clearly show the characteristic 421-, 548-, and 584-nm bands of ferrylmyoglobins. Relatively clean isosbestic points at several wavelengths in the spectrum support metmyoglobin and ferrylmyoglobins as the main absorbing species.

Mb–AQ films had a Soret band at 409 nm for MbFe(III) but the band at 503 nm was only a shoulder and a band at approximately 540 nm was also present. The spectra in the 500–650-nm range were somewhat different from MbFe(III) in solution, suggesting the possibility of conformation-changing interactions between the positively charged Mb and the anionic AQ. Upon electrolysis at -0.6 V, these films showed a 421 nm band only after 40 min (Fig. 5). While a band at 548 nm was found, the accompanying ferrylmyoglobin band at 584 nm was not clearly observed (Fig. 5b), and a band at approximately 570 was seen. These results are consistent with ferrylmyoglobins formed slowly in the Mb–AQ films, with the possibility of some decomposition resulting from exposure to H_2O_2 [8], or even the presence of a small amount of X–MbFe(II)–O_2. In the presence of styrene, 2-h electrolysis was required before the 421-nm ferrylmyoglobin band was observed (Fig. 6) because of the reaction with styrene. This spectrum with a shoulder at 409 nm suggests that some metmyoglobin remains.

Spectroelectrochemistry of Mb–DNA films (Fig. 8) at -0.6 V in the presence styrene showed that initially the 409-, 503-, and 632-nm bands for MbFe(III) are predominant, and nearly an hour is required before the 421-, 548-, 584-nm bands of ferrylmyoglobins become the main spectral features. This conversion is much slower than in the absence of styrene (cf. Fig. 7) because ferrylmyoglobin radical is used up by oxidizing styrene, regenerating MbFe(III). The small amount of H_2O_2 formed initially presumably converts some MbFe(III) to $^{\bullet}$X–MbFe(IV)=O, but this species disappears quickly as it reacts with styrene. As H_2O_2 concentration builds up with time (cf. Fig. 9), ferrylmyoglobin formation becomes more rapid and metmyoglobin peaks begin to decrease as ferrylmyoglobin peaks increase. After electrolysis

for 60 min, the majority of the Mb in the film resides in ferrylmyoglobin forms.

At the 60-min point in this experiment, the applied potential was changed to −0.1 V, where MbFe(III) is not reduced (Fig. 8). H_2O_2 is no longer being produced at this voltage, and it is gradually used up in Mb-mediated oxidation of styrene (cf. Fig. 9). Eventually, the H_2O_2 concentration falls low enough so that MbFe(III) can again predominate, as shown by characteristic 409-, 503-, 632-nm bands after 120 min (Fig. 8). Since ferrylmyoglobins are strong oxidants, it is also possible that their electrochemical reduction plays a role in this complex reaction process.

A remarkable feature of this experiment in DNA films at room temperature is that very little decomposition of Mb seems to have taken place. The maximum Soret band at 120 min for MbFe(III) is about the same as the maximum in the early stages of the experiment (Fig. 8). In solution [26] or in ultrathin polyion films [27], oxidation of styrene for 1 h by aerobic electrolysis at 4°C results in decomposition of 20% or more of the protein. Decomposition of Mb from reaction of amino acid residues with H_2O_2 also occurs in solution [8]. The stability of Mb in Mb–DNA films may suggest a special protective role for DNA in this reaction.

Formation of ferrylmyoglobin and its reaction with styrene in AQ and DNA films can be rationalized by the pathway in Scheme 1, similar to that proposed for Mb in solutions and microemulsions [26]:

$$\text{X–MbFe(III)} + e^- \rightleftharpoons \text{X–MbFe(II)} \quad \text{(at electrode)} \tag{3}$$

$$\text{X–MbFe(II)} + O_2 \rightarrow \text{X–MbFe(II)–O}_2 \tag{4}$$

$$\text{X–MBFe(II)} - O_2 + 2e^- + 2H^+ \rightarrow \text{X–MbFe(II)} + H_2O_2 \quad \text{(at electrode)} \tag{5}$$

$$\text{X–MbFe(III)} + H_2O_2 \rightarrow {}^{\bullet}\text{X–MbFe(IV)=O} + H_2O \tag{1′}$$

$${}^{\bullet}\text{X–MbFe(IV)=O} + \text{ArCH=CH}_2 \rightarrow \text{X–MbFe(III)} + \text{ArCHOCH}_2 \tag{6}$$

To initiate the reaction, an electron from the electrode first reduces metmyoglobin [Eq. (3)] in the film to X–MbFe(II), which reacts rapidly with oxygen to give X–MbFe(II)–O_2 [Eq. (4)], a reaction with rate constant $2 \times 10^7\ M^{-1}\ s^{-1}$ [35].

Hydrogen peroxide is formed by electrochemical reduction of X–MbFe(II)–O_2 [Eq. (5)], as demonstrated in solution [26]. A catalytic cycle involving Eqs. (4) and (5) is suggested by large reduction currents in the presence of oxygen at the potentials of MbFe(III) reduction, and also supported by the finding of significantly more hydrogen peroxide after electrolysis with electrodes coated with Mb films compared to controls with no protein present (Fig. 9). Auto-oxidation of X–MbFe(II)–O_2 with rate constant [35] $2 \times 10^{-6}\ s^{-1}$ is too slow to be important in catalytic production of H_2O_2.

Ferrylmyoglobin radical ${}^{\bullet}$X–MbFe(IV)=O is produced by reaction of H_2O_2 formed during electrolysis with X–MbFe(III) uncoupled to the electrode reaction. Choe et al. [4] showed that styrene is oxidized by ${}^{\bullet}$X–MbFe(IV)=O, but not by non-radical MbFe(IV)=O. Thus, ${}^{\bullet}$X–MbFe(IV)=O transfers its oxygen to styrene to give styrene oxide and X–MbFe(III) [Eq. (6)]. This is the second catalytic cycle in the 'doubly catalytic' pathway, since the X–MbFe(III) produced in Eq. (6) feeds back into Eq. (3) to begin the entire oxygen reduction/styrene oxidation sequence over again. Thus, Mb-catalyzed electrochemical *reduction* of oxygen results in Mb-catalyzed *oxidation* of styrene.

There is a second pathway for Mb–H_2O_2 oxidation of olefins that involves reaction of O_2 with a radical site on the ${}^{\bullet}$X–MbFe(IV)=O surface, yielding an amino acid-peroxyl radical that also can oxidize styrene [1–4]. A surface amino acid radical is also involved in H_2O_2-initiated dimerization of Mb [8]. The significance of these radical pathways in the DNA and AQ films cannot be ascertained from the present results. However, we might speculate that the better stability of

Mb–DNA films during electrolysis could be related in some way to the relative importance of the ferrylmyoglobin pathway vs. the radical oxidation pathway.

5. Conclusions

Cast Mb–DNA and Mb–AQ films catalyze electrochemically-driven styrene oxidation via a ferrylmyoglobin radical intermediate. Ferrylmyoglobin formation in Mb–DNA films is much faster and occurs with less Mb decomposition compared to Mb–AQ films. The better performance of Mb–DNA films is correlated with a larger fraction of electroactive Mb and better stability than for the Mb–AQ films. While ferrylmyoglobin radical may be involved in oxidative cell damage [5,20–23], the significance of interactions with polyelectrolytes in vivo is unknown.

Acknowledgements

This work was supported by grant No. ES03154 from the US National Institute of Environmental Health Sciences (NIEHS), NIH. Contents are solely the responsibility of the authors and do not necessarily represent official views of NIEHS, NIH. The authors thank CVI Spectral Instruments for the loan of a CCD spectrometer.

References

[1] P.R. Ortiz de Montellano, C.E. Catalano, Epoxidation of styrene by hemoglobin and myoglobin, J. Biol. Chem. 260 (1985) 9265–9271.

[2] S.I. Rao, A. Wilks, P.R. Ortiz de Montellano, The roles of His-64, Tyr-103, Tyr-146, and Tyr-151 in the epoxidation of styrene and β-methylstyrene by recombinant sperm whale myoglobin, J. Biol. Chem. 268 (1993) 803–809.

[3] P.R. Ortiz de Montellano, S.I. Rao, A. Wilks, Mechanisms of myoglobin as an oxidative catalyst, Life Chem. Rep. 12 (1994) 29–32.

[4] Y.S. Choe, S.I. Rao, P.R. Ortiz de Montellano, Requirement of a second oxidation equivalent for ferryl oxygen transfer to styrene in the epoxidation catalyzed by myoglobin–H_2O_2, Arch. Biochem. Biophys. 314 (1994) 126–131.

[5] A. Arduini, L. Eddy, P. Hochstein, The reduction of ferryl myoglobin by ergothioneine, Arch. Biochem. Biophys. 281 (1990) 41–43.

[6] S.I. Rao, A. Wilks, M. Hamberg, P.R. Ortiz de Montellano, The lipoxygenase activity of myoglobin, J. Biol. Chem. 269 (1994) 7210–7216.

[7] D.J. Kelman, J.A. DeGray, R.P. Mason, Reaction of myoglobin with hydrogen peroxide forms a peroxyl radical which oxidizes substrates, J. Biol. Chem. 269 (1994) 7458–7563.

[8] R.A. Tschirret-Guth, P.R. Ortiz de Montellano, Protein radicals in myoglobin dimerization and myoglobin-catalyzed styrene epoxidation, Arch. Biochem. Biophys. 335 (1996) 93–101.

[9] P. George, D.H. Irvine, The reaction between metmyoglobin and hydrogen peroxide, Biochem. J. 52 (1952) 511–516.

[10] N.K. King, M.E. Winfield, The mechanism of metmyoglobin oxidation, J. Biol. Chem. 238 (1963) 1520–1528.

[11] N.K. King, M.E. Winfield, Products of metmyoglobin oxidation at acid pH, Aust. J. Biol. Sci. 19 (1966) 211–217.

[12] T. Yonetoni, H. Schleyer, Studies on cytochrome *c* peroxidase. IX. The reaction of ferrimyoglobin with hydroperoxides and a comparison of peroxide-induced compounds of ferrimyoglobin and cytochrome *c* peroxidase, J. Biol. Chem. 242 (1966) 1974–1979.

[13] J.F. Gibson, D.J.E. Ingram, P. Nicholls, Free radical produced in the reaction of metmyoglobin with hydrogen peroxide, Nature 181 (1958) 1398–1399.

[14] J.J.O. Turner, C.A. Rice-Evans, M.J. Davies, E.S.R. Newman, Free radicals, myocytes, and reperfusion injury, Biochem. Soc. Trans. 18 (1990) 1056–1059.

[15] A.J. Sitter, C.M. Reczek, J. Terner, Observation of the $Fe^{IV}=O$ stretching vibration of ferryl myoglobin by resonance Raman spectroscopy, Biochem. Biophys. Acta 828 (1985) 229–235.

[16] M. Chance, L. Powers, C. Kumar, B. Chance, X-ray absorption studies of myoglobin peroxide reveal functional differences between globins and heme enzymes, Biochemistry 25 (1985) 1259–1265.

[17] C.E. Schulz, R. Chiang, P.G. Debrunner, Mossbauer parameters of Fe^{4+} heme proteins of spin $s=1$, J. Physique Colloque 40 (1979) C2534–C2536.

[18] N. Foote, P.M.A. Gadsby, C. Greenwood, A.J. Thomson, pH-dependent forms of the ferryl haem in myoglobin peroxide analyzed by variable-temperature magnetic circular dichrosim, Biochem. J. 261 (1979) 515–522.

[19] G.N. La Mar, J.S. De Ropp, L. Latos-Grazynski et al., Proton NMR characterization of the ferryl group in model heme complexes and hemoproteins: evidence for the $Fe^{IV}=O$ group in ferryl myoglobin and compound II of horseradish peroxidase, J. Am. Chem. Soc. 105 (1985) 782–787.

[20] M.J. Davies, Identification of a globin free radical in equine myoglobin treated with peroxides, Biochem. Biophys. Acta 1077 (1991) 86–90.

[21] C. Rice-Evans, The potential for free radical damage by myoglobin, in: A.E. Favier, J. Neve, P. Faure (Eds.), Trace Elements and Free Radicals in Oxidative Diseases, AOCS Press, Champaign, III, 1994, pp. 92–99.
[22] J.J.O. Turner, C.A. Rice-Evans, M.J. Davies, E.S.R. Newman, The formation of free radicals by cardiac myocytes under oxidative stress and the effects of electron donating drugs, Biochem. J. 277 (1991) 833–837.
[23] D. Galaris, E. Cadenas, P. Hochstein, Glutathione-dependent reduction of peroxides during ferryl- and metmyoglobin interconversion: a potential protective mechanism in muscle, Free Radical Biol. Med. 6 (1989) 473–478.
[24] J.B. Schenkman, H. Greim, Cytochrome P450, Springer-Verlag, Berlin, 1993.
[25] P.R. Ortiz de Montellano, Cytochrome P450, 2, Plenum, New York, 1995.
[26] A.C. Onuoha, X. Zu, J.F Rusling, Electrochemical generation and reactions of ferrylmyoglobin in water and microemulsions, J. Am. Chem. Soc. 119 (1997) 3979–3986.
[27] Y.M. Lvov, Z. Lu, J.B. Schenkman, X. Zu, J.F. Rusling, Direct electrochemistry of myoglobin and cytochrome $P450_{cam}$ in alternate polyion layer-by-layer films with DNA and other polyions, J. Am. Chem. Soc. 120 (1998) 4073–4080.
[28] A.-E.F. Nassar, W.S. Willis, J.F. Rusling, Electron transfer from electrodes to myoglobin: facilitated in surfactant films and blocked by adsorbed biomacromolecules, Anal. Chem. 67 (1995) 2386–2392.
[29] A.K. Bej, M.H. Mahbubani, in: C.A. Dangler (Ed.), Nucleic Acid Analysis, Wiley-Liss, New York, 1996, pp. 231–274.
[30] N. Hu, J.F. Rusling, Electrochemistry and catalysis with myoglobin in hydrated poly(ester sulfonic acid) ionomer films, Langmuir 13 (1997) 4119–4125.
[31] R.W. Murray, Chemically modified electrodes, in: A.J. Bard (Ed.), Electroanalytical Chemistry, 13, Marcel Dekker, New York, 1984, pp. 191–368.
[32] A.-E. Nassar, J.F. Rusling, N. Nakashima, Electron transfer between electrodes and heme proteins in protein–DNA films, J. Am. Chem. Soc. 118 (1996) 3043–3044.
[33] X. Zu, Z. Lu, Z. Zhang, J.B. Schenkman, J.F. Rusling, Electro-enzyme catalyzed oxidation of styrene and *cis*-β-methylstyrene using thin films of cytochrome P450cam and myoglobin, J. Am. Chem. Soc., submitted.
[34] J.F. Rusling, Enzyme bioelectrochemistry in cast biomembrane-like films, Acc. Chem. Res. 31 (1998) 363–369.
[35] T. Wazawa, A. Matsuoka, G. Tajima, Y. Sugawara, K. Nakamura, K. Shikama, Hydrogen peroxide plays a key role in the oxidation reaction of myoglobin by molecular oxygen, Biophys. J. 63 (1992) 544–550 and references therein.